Macromolecules

pubs.acs.org/Macromolecules

Article

Tuning Polyethylene Molecular Weight Distributions Using Catalyst Support Composition

Philip Kenyon, D. W. Justin Leung, Zoë R. Turner, Jean-Charles Buffet, and Dermot O'Hare*

Cite This: *Macromolecules* 2022, 55, 3408−3414

Read Online

ACCESS | Metrics & More | Article Recommendations | Supporting Information

ABSTRACT: Bimodal polyethylene is generated from a single immobilized catalyst on a single support under a single set of reaction conditions without introducing chain transfer agents. Using *rac*-ethylenebis(1-indenyl)zirconium dichloride [(EBI)$ZrCl_2$] immobilized on a nickel-containing layered double hydroxide (LDH) support produces two distinct molecular weight distributions. The ratio of these two distinct fractions can be tuned by varying the LDH support as well as by changing the reaction conditions.

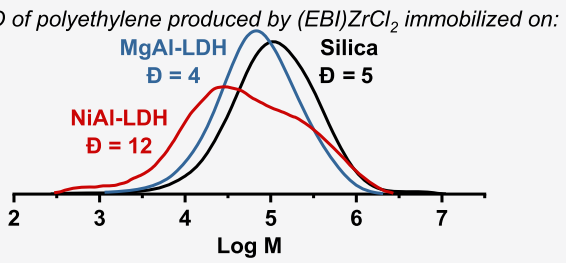

The material properties of a polymer are intrinsically linked to the molecular weight distribution (MWD) of the individual chains.[1] High molecular weight polyethylenes have high tensile strength and abrasion resistance,[2] while low molecular weight polyethylenes are easily processed due to a low melt viscosity[3] and rapid crystallization.[4] Blending of these polymers with distinct MWDs allows for tailoring of the material properties to allow for improved mechanical properties and/or enhanced processability.[5−8]

Classical polyethylene catalysts such as Ziegler−Natta and Phillips systems produce polymers with (very) broad MWDs due to the multisite nature of these catalysts. By comparison, the single site nature of metallocenes and other well-defined homogeneous catalysts produce narrow monomodal MWDs, where one catalyst produces one polymer material.[9]

Tuning a single well-defined catalyst to produce multiple polymer microstructures under different conditions is therefore of considerable academic and industrial interest.[10−12] Solvents can play a key role through influencing ion pairs,[13] directly interacting with the metal center,[14] or inducing the formation of clusters with multiple centers.[15,16] Addition of species such as chain-transfer agents,[17−19] reducing and oxidizing agents,[20−22] Lewis acids and metal salts,[23−27] and polar additives[28,29] can allow for the production of distinct polymer architectures from a single catalyst precursor.

However, for industrial gas- or slurry-phase polymerization, many of these methods are not yet commercially realized. Instead, polymer blends are either produced by using reactor cascades or by using blends of catalysts.[30,31] Catalyst blends can be used in solution[32] but are typically immobilized on a single support. Using two or more catalysts on a single support can allow for the production of polymers with unique material properties;[33] however, care must be taken that the two catalysts do not affect one another in a detrimental fashion.[34]

Recently, Mülhaupt and co-workers demonstrated that by varying the amount of methylaluminoxane (MAO) used to immobilize a chromium catalyst, distinct MWDs could be obtained.[35] A conceptually similar approach would be to create a support with a range of sites, so that one metallocene might behave in very different ways when immobilized on the surface. A classical support for immobilizing metallocenes is silica, often by using MAO as a cocatalyst.[36,37] Silica lacks significant chemical tunability, with typical methods focusing on controlling the surface silanol concentrations by calcination,[38] control of the physical properties such as pore size,[39] and reactions with surface silanols.[40,41]

By contrast, layered double hydroxides (LDHs) are a class of highly tunable inorganic materials with the chemical composition $[M_{1-x}M'_x(OH)_2]^{y+}[A^{n-}_{n/y}]\cdot z(H_2O)$, consisting of layers of brucite-like metal hydroxides containing a mixture of divalent (M) and trivalent (M′) metal ions in varying ratios ($0 < x < 1$), with anions (A) intercalated between the layers to balance the charge.

The concentration of hydroxide groups at the surface can be controlled by calcination,[42] and they have previously been used as supports for slurry-phase polymerization.[43−45] They can also be templated onto silica[46,47] and other inorganic materials,[48,49] and these core−shells have also been used as supports for polymerization catalysis.[50]

Here we demonstrate the potential of this tunable support by varying the metallic composition of the LDH; this radically

Received: December 22, 2021
Revised: February 21, 2022
Published: April 22, 2022

changes the molecular weight distribution of the polyethylene produced by *rac*-ethylenebis(1-indenyl)zirconium dichloride [(EBI)$ZrCl_2$] immobilized on these supports. Two series of LDHs were produced by a coprecipitation method, where the theoretical ratio of M^{2+}:Al^{3+} was fixed at 2:1 ($Ni_x(Mg_{2-x})Al$) and 3:1 ($Ni_x(Mg_{3-x})Al$). In these series, the nickel content was varied while other factors such as the coprecipitation pH (pH 10) and the intercalated anion (CO_3^{2-}) were fixed. To ensure all LDH supports had a large surface area, they underwent an aqueous miscible solvent treatment by stirring in ethanol for 4 h.[51] $Ni_x(Mg_{2-x})Al$ and $Ni_x(Mg_{3-x})Al$ can therefore be represented by the general formulas $Ni_x(Mg_{2-x})Al(OH)_6(CO_3)_{0.5}(H_2O)_y(C_2H_5OH)_z$ and $Ni_x(Mg_{3-x})Al(OH)_8(CO_3)_{0.5}(H_2O)_y(C_2H_5OH)_z$, respectively.

The purity of the LDH can be seen in the XRD powder patterns ($Ni_x(Mg_{2-x})Al$ shown in Figure 1; for $Ni_x(Mg_{3-x})Al$ see the Supporting Information; the TGA curves ($Ni_x(Mg_{2-x})Al$ are shown in Figure 2; for $Ni_x(Mg_{3-x})Al$ and DTGA curves for all samples, see the Supporting Information) and the good agreement between the theoretical and actual nickel contents (Table 1).

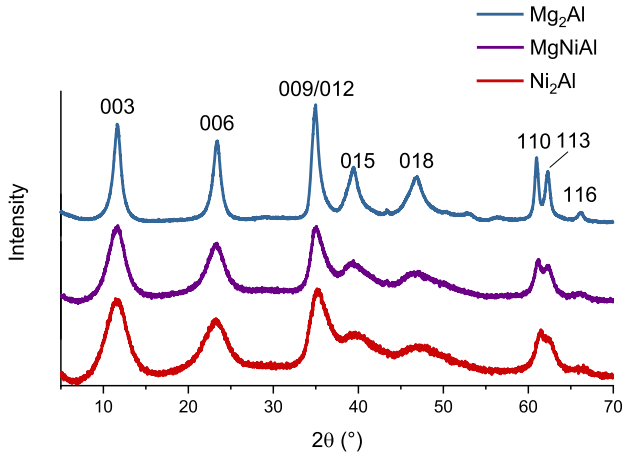

Figure 1. XRD powder patterns of $Ni_x(Mg_{2-x})Al$ LDH.

The XRD powder patterns show the expected Bragg reflections associated with a crystalline LDH. There is a small shift in position of the 110 Bragg reflection to higher 2θ values as the Ni^{2+} content is increased. This is observed for both the $Ni_xMg_{3-x}Al$ and the $Ni_xMg_{2-x}Al$ series and is consistent with a decrease in the average metal−metal distance (Table 1) as the larger Mg^{2+} ion is replaced with the smaller Ni^{2+} ion.[52] The *a* lattice parameters for both $Ni_xMg_{3-x}Al$ and the $Ni_xMg_{2-x}Al$ vary linearly with Ni^{2+} content (Vegard's law) (Figure S2), thus indicating they form solid solution phases.

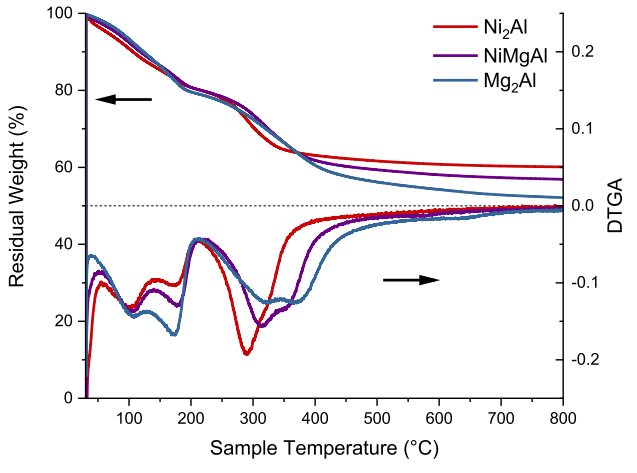

Figure 2. TGA curves of $Ni_x(Mg_{2-x})Al$ LDH.

The TGA curves show the expected weight losses associated with calcination of an LDH. Below 200 °C, there is loss of interlayer solvent molecules (ethanol and water) seen as distinct maxima in the DTGA at approximately 90 and 170 °C, respectively. As the nickel content changes the ratio between these two peaks changes, suggesting a change in the composition of the interlayer solvents. Above 200 °C, dehydroxylation of OH bonds in the LDH occurs; this is associated with the partial loss of the carbonate anion and formation of semiamorphous mixed metal oxides (also called layered double oxides, LDO).[53,54] The dehydroxylation temperature has been previously shown to be dependent on the nature of the $M(OH)M_2$ sites (among other factors), and as nickel content increases, the dehydroxylation temperature decreases.[55] For both series as the nickel content increases, the residual weight at 800 °C increases as the magnesium ions are replaced by heavier nickel ions.

Importantly, the residual weight at 800 °C correlates with the theoretical Ni^{2+} content (Figure S5), suggesting there are no amorphous impurities in the samples which were not observed in the powder XRD patterns. In combination these measurements suggest that the nickel supports are synthetically pure and suitable for use in studying the influence of the nickel content on polymerization.

To generate an appropriate mixed metal oxide support, the LDH were calcined at 400 °C under vacuum for 3 h.[53,54] The resulting Layered Double Oxide (LDO) was then treated with *d*-MAO (40 wt %), and (EBI)$ZrCl_2$ was immobilized onto the support. Polymerizations were performed by using hexanes as the diluent and triisobutylaluminum (TiBA) as a scavenger. A silica-based catalyst support (PQ-ES70X) calcined at 400 °C for 6 h was also used for comparison purposes.

All catalysts were active for ethylene polymerization; no clear trend was observed for the influence of nickel content on productivity, but all catalysts were more active than the silica reference under the conditions used here (see Table S1 for full details of all polymerizations). However, the dramatic change comes in the MWD of the polymer produced. While a broad MWD (M_w/M_n > 5) is obtained for nearly all the supports used here, a much broader MWD can be obtained for the LDO series containing nickel, especially at higher temperatures.

While an approximately monomodal MWD is obtained for all catalysts at 70 °C (see Figure 3 for an example), catalysts based on supports with a high nickel content (e.g., Ni_2Al) have clearly become bimodal at 90 °C, while those based on nickel-free LDO supports (Mg_2Al and Mg_3Al) and the silica reference retain their monomodal distribution (see Figure 4). Note that all these distributions are consistent with a multisite catalyst as can be shown by deconvolution of the narrowest (M_w/M_n = 3.6) and broadest (M_w/M_n = 12.4) MWDs into multisite models (5 and 7 sites, respectively). For this reason, it was decided to represent the broadening of the MWDs simply in terms of M_w/M_n (for more details on the deconvolution see the Supporting Information).

Polymerization of ethylene using nickel and other late-transition-metal catalysts is well established. A range of molecular weights can be produced; however, they are typically

https://doi.org/10.1021/acs.macromol.1c02604
Macromolecules 2022, 55, 3408−3414

Table 1. LDH Supports Synthesized in This Study and Their Composition

support sample name	theoretical Ni:Mg ratio[a]	actual Ni:Mg ratio[b]	theoretical M(II) Ni content (%)[c]	actual M(II) Ni content (%)[d]	residual weight at 800 °C (%)[e]	metal−metal distance (Å)[f]
Mg_2Al	0:2	0:1.82	0	0	52.1	3.0362
NiMgAl	1:1	0.98:0.99	50	49.6	56.9	3.0302
Ni_2Al	2:0	1.95:0	100	100	60.1	3.0186
Mg_3Al	0:3	0:2.87	0	0	52.4	3.0576
$NiMg_2Al$	1:2	0.94:1.92	33.3	32.9	55.7	3.0546
Ni_2MgAl	2:1	1.92:0.96	66.7	66.8	58.9	3.0470
Ni_3Al	3:0	2.89:0	100	100	62.3	3.0408

[a]Based on molar ratios of metal nitrates used in the synthesis, relative to Al. [b]Determined by ICP-MS, relative to Al. [c]Based on ratios of metal nitrates used in the synthesis. [d]As determined by ICP-MS. [e]As determined by TGA, 30−800 °C, 5 K min^{-1}. [f]Determined from the position of 110 Bragg reflection in the XRD powder pattern.

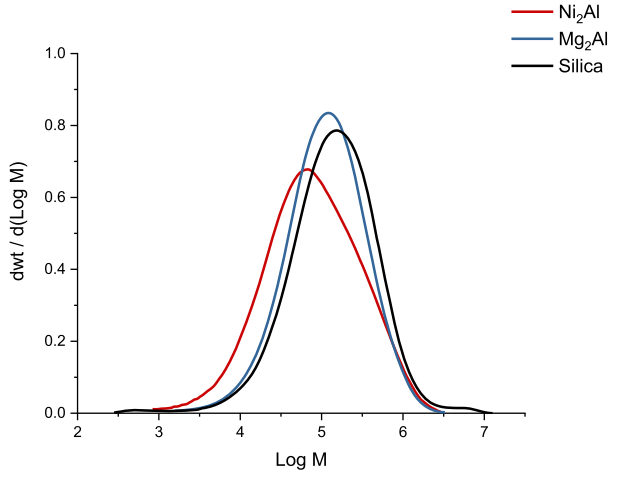

Figure 3. MWD of polyethylene produced by using two selected catalysts based on Ni_2Al and Mg_2Al LDOs and the silica reference at 70 °C.

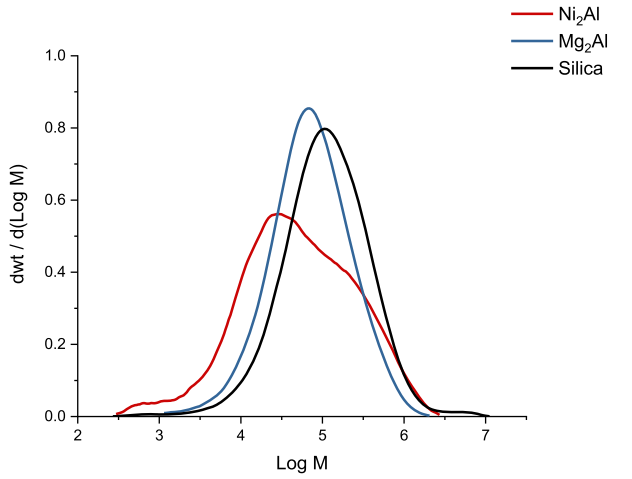

Figure 4. MWD of polyethylene produced by using two selected catalysts based on Ni_2Al and Mg_2Al LDOs and the silica reference at 90 °C.

lower than those produced by metallocene catalysts due to their propensity for β-H elimination and chain transfer, which must be suppressed via sophisticated catalyst design.[56−61] This propensity for β-H elimination also leads to nickel-based catalysts often producing highly branched polyethylene via chain-walking processes.[62] By contrast, the polymers produced here are clearly linear and display sharp melting and crystallization curves with peak melting temperatures typical of HDPE produced by metallocenes, even when a clearly bimodal polyethylene is produced (Figure 5). Reference

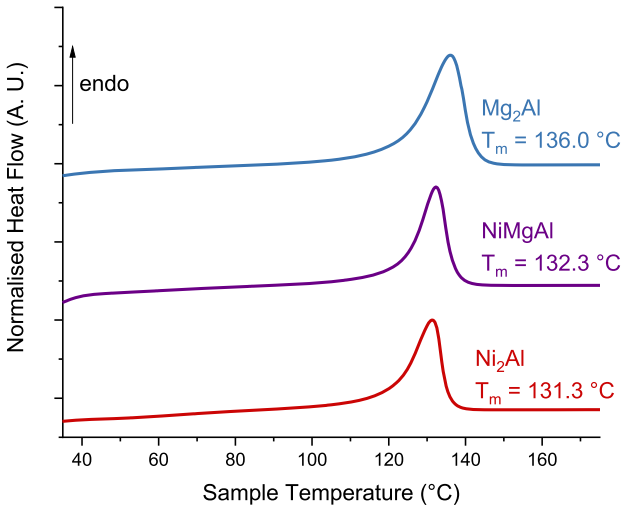

Figure 5. DSC of polyethylene produced by using selected catalysts based on Mg_2Al, NiMgAl, and Ni_2Al LDO supports at 90 °C.

experiments performed at 90 °C using the support prior to the immobilization of the metallocene did not produce polyethylene, clearly demonstrating the role of the zirconocene in producing the low molecular weight fraction (see Table S2 for more details).

This bimodality is clearly temperature sensitive (see Figure 6), but it can also be tuned by the nickel content of the support (see Figures 6 and 7). As the nickel content is increased, the bimodality increases; as is indicated by the change in dispersity (M_w/M_n), this triples from ∼4 (for Mg_2Al) to over 12 (for a Ni_2Al LDO support at 90 °C).

Clearly, when (EBI)$ZrCl_2$ is immobilized on an LDO containing nickel, a lower molecular weight fraction is produced. This low molecular weight fraction must still be generated by the metallocene and is likely the result of a distinct ion pair forming under polymerization conditions, which has distinct reactivity with (for example) the scavenger TiBA. The influence of ion pairing on the kinetics of olefin polymerization has been extensively demonstrated by using well-defined activators,[63−67] and it has been shown that different types of MAO produce distinct cation−anion pairs which undergo termination via transfer to aluminum alkyls at different rates.[68]

https://doi.org/10.1021/acs.macromol.1c02604
Macromolecules 2022, 55, 3408−3414

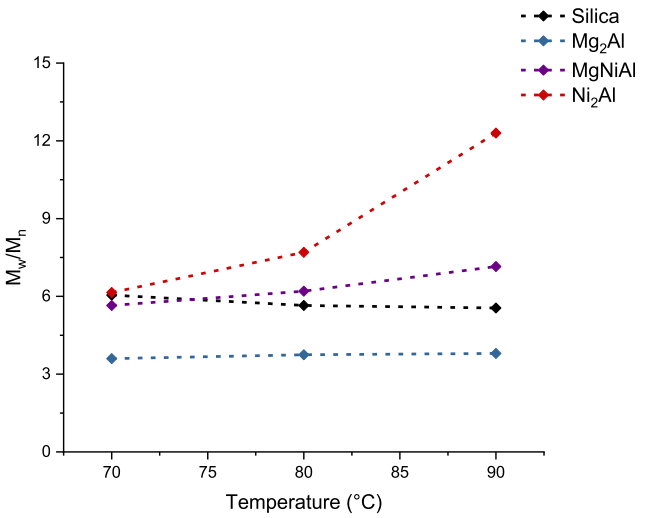

Figure 6. Change in dispersity (M_w/M_n) with temperature for catalysts based on $Ni_x(Mg_{2-x})Al$ LDO supports. The reference catalyst based on a silica support is also included.

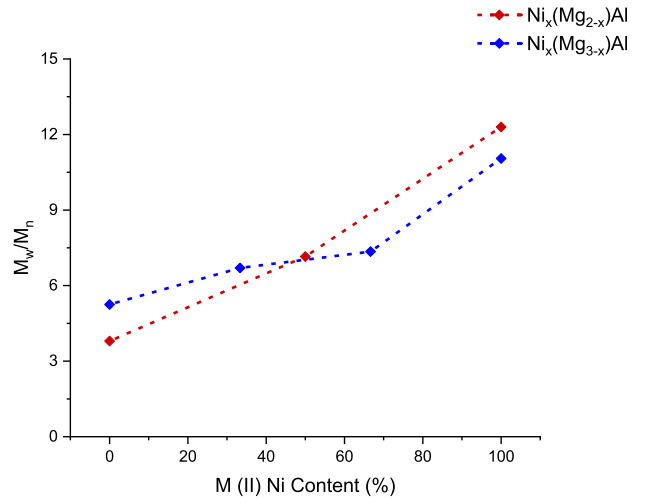

Figure 7. Change in dispersity (M_w/M_n) at 90 °C showing an increase with increasing nickel content for catalysts based on $Ni_x(Mg_{2-x})Al$ and $Ni_x(Mg_{3-x})Al$ LDO supports.

The Lewis acidity of the support has been previously shown to influence how MAO and aluminum alkyls bind to protic supports,[69] while interactions with the support may influence the stability of MAO species, the barrier to activation, and the cation−anion separation for MAO/metallocene ion pairs.[70] Recently, we demonstrated that the Lewis acidity of an LDO surface can increase the productivity of (EBI)$ZrCl_2$ immobilized using MAO by influencing the ion-pairing.[71] This Lewis acidity can be shown by a change in the absorption of NH_3, from binding solely via hydrogen bonds ("type A" sites) to incorporating both a hydrogen bond and a dative bond ("type B" sites, see Figure 8).[72]

Upon comparison of the TPD profiles of $Ni_x(Mg_{2-x})Al$ LDO, it is apparent that there is a dramatic change in the Lewis acidity of the supports. While for Mg_2Al most of the ammonia is bound via hydrogen bonds, the contribution of Lewis acidic sites increases dramatically with the nickel content (Figure 9). The amount of ammonia bound by the LDO increases with nickel content, from 0.22 to 0.69 mmol g^{-1}, and Ni_2Al binds ammonia more strongly, reflected in the higher

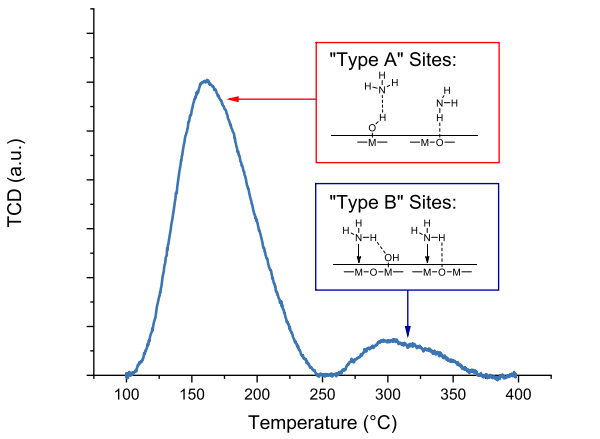

Figure 8. Temperature-programmed desorption of ammonia from the surface of Mg_2Al LDO, showing the distinct types of sites.

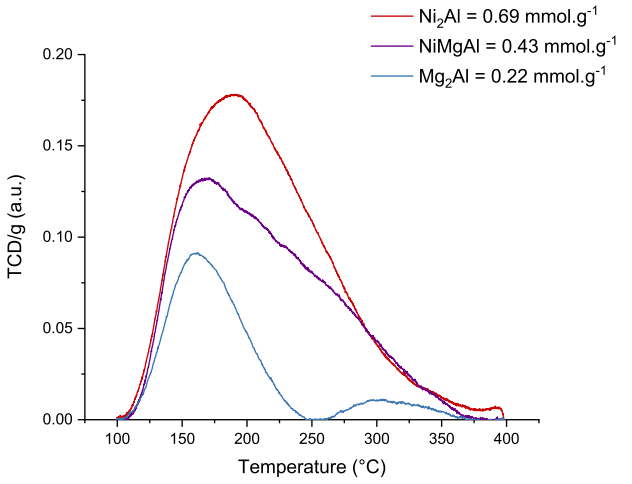

Figure 9. Temperature-programmed desorption of ammonia from the surfaces of $Ni_x(Mg_{2-x})Al$ LDOs, showing a significant increase in the ammonia bound via Lewis acidic "type B" sites for high nickel content LDOs.

peak desorption temperature (171 and 190 °C for NiMgAl and Ni_2Al, respectively) and more desorption occurring at temperatures above 200 °C.

Deconvolution of these curves suggests that for $Ni_x(Mg_{2-x})Al$ this is associated with an increase from 0.03 to 0.44 mmol g^{-1} of ammonia being bound via type B sites (Figure 10; see the Supporting Information for more details about the deconvolution of TPD curves). These results are consistent with previous studies which show that nickel, in contrast to magnesium, can contribute to the overall Lewis acidity of the LDO.[72]

Clearly the presence of a high number of acidic sites influences the anionic structure of the MAO on the surface. Further characterization of these changes is challenging due to poorly defined structures of both the LDO support and the MAO used to react with the surface and the low amount of zirconocene used (0.5 wt %). The paramagnetic nature and intense coloration of the nickel-containing supports also prevent the use of ssNMR and DR−UV−vis techniques. However, we can assume that these changes influence the ion pairs formed when the zirconocene [(EBI)$ZrCl_2$] reacts with the support. Different ion pairs will have not only different rates of reaction with the scavenger (TiBA)[68] but also differing

https://doi.org/10.1021/acs.macromol.1c02604
Macromolecules 2022, 55, 3408−3414

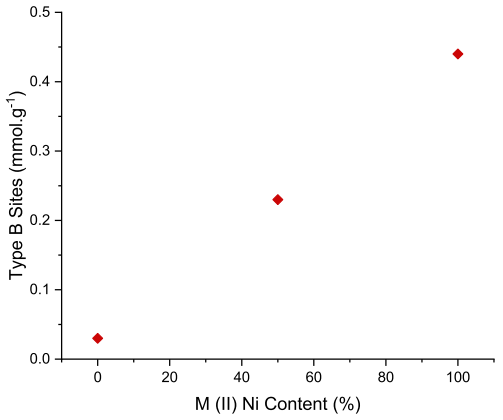

Figure 10. Amount of ammonia bound to the surfaces of $Ni_x(Mg_{2-x})$ Al LDOs via Lewis acidic "type B" sites.

activities.[71] Interestingly, the nickel-containing supports display enough chemical heterogeneity to produce ion pairs, which produce a high molecular weight polyethylene as well as new sites that readily react with TiBA to give a low molecular weight fraction.

In conclusion, incorporating nickel into an LDH-based support allows the generation of bimodal polyethylene in slurry-phase polymerization using *rac*-ethylenebis(1-indenyl) zirconium dichloride, a commercial metallocene catalyst on a single support. This results from an extreme change in the Lewis acidity of the support surface. This bimodality can be tuned by the degree of nickel in the support and is also influenced by polymerization temperature. This approach of using the chemical tunability of a support to influence the polymer produced allows for an easily adopted approach to produce distinct polymer blends using a single catalyst under a single set of conditions.

■ ASSOCIATED CONTENT

Supporting Information

The Supporting Information is available free of charge at https://pubs.acs.org/doi/10.1021/acs.macromol.1c02604.

Synthetic procedures for LDH, calcined LDH (LDO), catalyst supports and catalysts; polymerization procedure; XRD, TGA, and DTGA analysis of $Ni_xMg_{3-x}Al$; plots of unit cell parameter *a* against LDH nickel content; plots of residual weight against LDH nickel content; polymerization data; procedure for reference polymerizations; GPC traces of all polyethylene samples; deconvolutions of GPC traces for the broadest and narrowest MWD polyethylene samples; TPD curves for all LDO; deconvolutions of TPD curves (PDF)

■ AUTHOR INFORMATION

Corresponding Author

Dermot O'Hare − *Chemistry Research Laboratory, Department of Chemistry, University of Oxford, Oxford OX1 3TA, U.K.;* orcid.org/0000-0001-8054-8751; Email: dermot.ohare@chem.ox.ac.uk

Authors

Philip Kenyon − *Chemistry Research Laboratory, Department of Chemistry, University of Oxford, Oxford OX1 3TA, U.K.;* orcid.org/0000-0003-0244-1347

D. W. Justin Leung − *Chemistry Research Laboratory, Department of Chemistry, University of Oxford, Oxford OX1 3TA, U.K.*

Zoë R. Turner − *Chemistry Research Laboratory, Department of Chemistry, University of Oxford, Oxford OX1 3TA, U.K.;* orcid.org/0000-0003-2044-9203

Jean-Charles Buffet − *Chemistry Research Laboratory, Department of Chemistry, University of Oxford, Oxford OX1 3TA, U.K.;* orcid.org/0000-0003-2062-9546

Complete contact information is available at: https://pubs.acs.org/10.1021/acs.macromol.1c02604

Notes

The authors declare no competing financial interest.

■ ACKNOWLEDGMENTS

Funding by SCG Chemicals Co., Ltd., is gratefully acknowledged. We thank Dr. Chunping Chen and Ms. Meng Lyu (University of Oxford) for XRD and TGA measurements. Ms. Liv Thobru and Ms. Sara Herum (AS Norner) are thanked for GPC measurements.

■ REFERENCES

(1) Nunes, R. W.; Martin, J. R.; Johnson, J. F. Influence of molecular weight and molecular weight distribution on mechanical properties of polymers. *Polym. Eng. Sci.* **1982**, *22* (4), 205−228.

(2) Tervoort, T. A.; Visjager, J.; Smith, P. On Abrasive Wear of Polyethylene. *Macromolecules* **2002**, *35* (22), 8467−8471.

(3) Kazatchkov, I. B.; Hatzikiriakos, S. G.; Bohnet, N.; Goyal, S. K. Influence of molecular structure on the rheological and processing behavior of polyethylene resins. *Polym. Eng. Sci.* **1999**, *39* (4), 804−815.

(4) Jeremic, D. Polyethylene. In *Ullmann's Encyclopedia of Industrial Chemistry*; Elvers, B., Ed.; Wiley-VCH: 2014; pp 1−42.

(5) Stürzel, M.; Mihan, S.; Mülhaupt, R. From Multisite Polymerization Catalysis to Sustainable Materials and All-Polyolefin Composites. *Chem. Rev.* **2016**, *116* (3), 1398−1433.

(6) Hees, T.; Zhong, F.; Koplin, C.; Jaeger, R.; Mülhaupt, R. Wear resistant all-PE single-component composites via 1D nanostructure formation during melt processing. *Polymer* **2018**, *151*, 47−55.

(7) Böhm, L. L.; Enderle, H. F.; Fleißner, M. High-density polyethylene pipe resins. *Adv. Mater.* **1992**, *4* (3), 234−238.

(8) Sifri, R. J.; Padilla-Velez, O.; Coates, G. W.; Fors, B. P. Controlling the Shape of Molecular Weight Distributions in Coordination Polymerization and Its Impact on Physical Properties. *J. Am. Chem. Soc.* **2020**, *142* (3), 1443−1448.

(9) Sauter, D. W.; Taoufik, M.; Boisson, C. Polyolefins, a Success Story. *Polymers* **2017**, *9* (6), 185−198.

(10) Sita, L. R. Ex Uno Plures ("Out of One, Many"): New Paradigms for Expanding the Range of Polyolefins through Reversible Group Transfers. *Angew. Chem., Int. Ed.* **2009**, *48* (14), 2464−2472.

(11) Hustad, P. D. Frontiers in olefin polymerization: reinventing the world's most common synthetic polymers. *Science* **2009**, *325* (5941), 704−707.

(12) Tran, T. V.; Do, L. H. Tunable modalities in polyolefin synthesis via coordination insertion catalysis. *Eur. Polym. J.* **2021**, *142*, 110100−11013.

(13) Gao, Y.; Chen, J.; Wang, Y.; Pickens, D. B.; Motta, A.; Wang, Q. J.; Chung, Y.-W.; Lohr, T. L.; Marks, T. J. Highly branched polyethylene oligomers via group IV-catalysed polymerization in very nonpolar media. *Nat. Catal.* **2019**, *2* (3), 236−242.

(14) Kenyon, P.; Falivene, L.; Caporaso, L.; Mecking, S. Ancillary Ligands Impact Branching Microstructure in Late-Transition-Metal Polymerization Catalysis. *ACS Catal.* **2019**, *9* (12), 11552−11556.

(15) Guironnet, D.; Rünzi, T.; Göttker-Schnetmann, I.; Mecking, S. Control of molecular weight in Ni(II)-catalyzed polymerization via the reaction medium. *Chem. Commun.* **2008**, No. 40, 4965−4967.
(16) Wei, J.; Shen, Z.; Filatov, A. S.; Liu, Q.; Jordan, R. F. Self-Assembled Cage Structures and Ethylene Polymerization Behavior of Palladium Alkyl Complexes That Contain Phosphine-Bis-(arenesulfonate) Ligands. *Organometallics* **2016**, *35* (20), 3557−3568.
(17) Britovsek, G. J. P.; Cohen, S. A.; Gibson, V. C.; Maddox, P. J.; van Meurs, M. Iron-Catalyzed Polyethylene Chain Growth on Zinc: Linear α-Olefins with a Poisson Distribution. *Angew. Chem., Int. Ed.* **2002**, *41* (3), 489−491.
(18) Arriola, D. J.; Carnahan, E. M.; Hustad, P. D.; Kuhlman, R. L.; Wenzel, T. T. Catalytic production of olefin block copolymers via chain shuttling polymerization. *Science* **2006**, *312* (5774), 714−719.
(19) Hyatt, M. G.; Guironnet, D. Silane as Chain Transfer Agent for the Polymerization of Ethylene Catalyzed by a Palladium(II) Diimine Catalyst. *ACS Catal.* **2017**, *7* (9), 5717−5720.
(20) Chen, M.; Yang, B.; Chen, C. Redox-Controlled Olefin (Co)Polymerization Catalyzed by Ferrocene-Bridged Phosphine-Sulfonate Palladium Complexes. *Angew. Chem., Int. Ed.* **2015**, *54* (51), 15520−15524.
(21) Anderson, W. C., Jr.; Rhinehart, J. L.; Tennyson, A. G.; Long, B. K. Redox-Active Ligands: An Advanced Tool To Modulate Polyethylene Microstructure. *J. Am. Chem. Soc.* **2016**, *138* (3), 774−777.
(22) Zhao, M.; Chen, C. Accessing Multiple Catalytically Active States in Redox-Controlled Olefin Polymerization. *ACS Catal.* **2017**, *7* (11), 7490−7494.
(23) Tanabiki, M.; Tsuchiya, K.; Motoyama, Y.; Nagashima, H. Monometallic and heterobimetallic azanickellacycles as ethylene polymerization catalysts. *Chem. Commun.* **2005**, No. 27, 3409−3411.
(24) Cai, Z.; Xiao, D.; Do, L. H. Fine-Tuning Nickel Phenoxyimine Olefin Polymerization Catalysts: Performance Boosting by Alkali Cations. *J. Am. Chem. Soc.* **2015**, *137* (49), 15501−15510.
(25) Basbug Alhan, H. E.; Jones, G. R.; Harth, E. Branching Regulation in Olefin Polymerization via Lewis Acid Triggered Isomerization of Monomers. *Angew. Chem., Int. Ed.* **2020**, *59* (12), 4743−4749.
(26) Tan, C.; Qasim, M.; Pang, W.; Chen, C. Ligand−metal secondary interactions in phosphine−sulfonate palladium and nickel catalyzed ethylene (co)polymerization. *Polym. Chem.* **2020**, *11* (2), 411−416.
(27) Smith, A. J.; Kalkman, E. D.; Gilbert, Z. W.; Tonks, I. A. $ZnCl_2$ Capture Promotes Ethylene Polymerization by a Salicylaldiminato Ni Complex Bearing a Pendent 2,2′-Bipyridine Group. *Organometallics* **2016**, *35* (15), 2429−2432.
(28) Zhang, Y.; Jian, Z. Polar Additive Triggered Branching Switch and Block Polyolefin Topology in Living Ethylene Polymerization. *Macromolecules* **2021**, *54* (7), 3191−3196.
(29) Jones, G. R.; Basbug Alhan, H. E.; Karas, L. J.; Wu, J. I.; Harth, E. Switching the Reactivity of Palladium Diimines with "Ancillary" Ligand to Select between Olefin Polymerization, Branching Regulation, or Olefin Isomerization. *Angew. Chem., Int. Ed.* **2021**, *60* (3), 1635−1640.
(30) Alt, F. P.; Böhm, L. L.; Enderle, H.-F.; Berthold, J. Bimodal polyethylene − Interplay of catalyst and process. *Macromol. Symp.* **2001**, *163* (1), 135−144.
(31) Liu, H.-T.; Davey, C. R.; Shirodkar, P. P. Bimodal polyethylene products from UNIPOL single gas phase reactor using engineered catalysts. *Macromol. Symp.* **2003**, *195* (1), 309−316.
(32) Mecking, S. Reactor blending with early/late transition metal catalyst combinations in ethylene polymerization. *Macromol. Rapid Commun.* **1999**, *20* (3), 139−143.
(33) Stürzel, M.; Hees, T.; Enders, M.; Thomann, Y.; Blattmann, H.; Mülhaupt, R. Nanostructured Polyethylene Reactor Blends with Tailored Trimodal Molar Mass Distributions as Melt-Processable All-Polymer Composites. *Macromolecules* **2016**, *49* (21), 8048−8060.
(34) Liu, H.; Bastiaansen, C. W. M.; Goossens, J. G. P.; Schenning, A. P. H. J.; Severn, J. R. Bimodal Ultrahigh Molecular Weight Polyethylenes Produced from Supported Catalysts: The Challenge of Using a Combined Catalyst System. *Macromol. Chem. Phys.* **2017**, *218* (5), 1600490−1600498.
(35) Zhong, F.; Thomann, R.; Mülhaupt, R. Tailoring Mono-, Bi-, and Trimodal Molar Mass Distributions and All-Hydrocarbon Composites by Ethylene Polymerization on Bis(imino)pyridine Chromium(III) Supported on Ultrathin Gibbsite Single Crystal Nanoplatelets. *Macromolecules* **2019**, *52* (7), 2701−2711.
(36) Severn, J. R.; Chadwick, J. C.; Duchateau, R.; Friederichs, N. "Bound but not gagged"-immobilizing single-site alpha-olefin polymerization catalysts. *Chem. Rev.* **2005**, *105* (11), 4073−4147.
(37) Severn, J. R. Methylaluminoxane (MAO), Silica and a Complex: The "Holy Trinity" of Supported Single-site Catalysts. In *Tailor-Made Polymers Via Immobilization of Alpha-Olefin Polymerization Catalysts*; Severn, J. R., Chadwick, J. C., Eds.; Wiley-VCH: 2008; pp 95−138.
(38) Bashir, M. A.; Vancompernolle, T.; Gauvin, R. M.; Delevoye, L.; Merle, N.; Monteil, V.; Taoufik, M.; McKenna, T. F. L.; Boisson, C. Silica/MAO/$(n\text{-BuCp})_2ZrCl_2$ catalyst: effect of support dehydroxylation temperature on the grafting of MAO and ethylene polymerization. *Catal. Sci. Technol.* **2016**, *6* (9), 2962−2974.
(39) Bunchongturakarn, S.; Jongsomjit, B.; Praserthdam, P. Impact of bimodal pore MCM-41-supported zirconocene/dMMAO catalyst on copolymerization of ethylene/1-octene. *Catal. Commun.* **2008**, *9* (5), 789−795.
(40) Barrera, E. G.; Stedile, F. C.; Brambilla, R.; dos Santos, J. H. Z. Broadening molecular weight polyethylene distribution by tailoring the silica surface environment on supported metallocenes. *Appl. Surf. Sci.* **2017**, *393*, 357−363.
(41) Barrera, E. G.; dos Santos, J. H. Z. Designing polyethylene characteristics by modification of the support for FI catalyst. *Mol. Catal.* **2017**, *434*, 1−6.
(42) Wright, C. M. R.; Ruengkajorn, K.; Kilpatrick, A. F. R.; Buffet, J.-C.; O'Hare, D. Controlling the Surface Hydroxyl Concentration by Thermal Treatment of Layered Double Hydroxides. *Inorg. Chem.* **2017**, *56* (14), 7842−7850.
(43) He, F. A.; Zhang, L. M. Organo-modified ZnAl layered double hydroxide as new catalyst support for the ethylene polymerization. *J. Colloid Interface Sci.* **2007**, *315* (2), 439−444.
(44) Buffet, J.-C.; Turner, Z. R.; Cooper, R. T.; O'Hare, D. Ethylene polymerisation using solid catalysts based on layered double hydroxides. *Polym. Chem.* **2015**, *6* (13), 2493−2503.
(45) Buffet, J.-C.; Wanna, N.; Arnold, T. A. Q.; Gibson, E. K.; Wells, P. P.; Wang, Q.; Tantirungrotechai, J.; O'Hare, D. Highly Tunable Catalyst Supports for Single-Site Ethylene Polymerization. *Chem. Mater.* **2015**, *27* (5), 1495−1501.
(46) Chen, C.; Felton, R.; Buffet, J.-C.; O'Hare, D. Core-shell SiO_2@LDHs with tuneable size, composition and morphology. *Chem. Commun.* **2015**, *51* (16), 3462−3465.
(47) Kwok, W. L. J.; Crivoi, D. G.; Chen, C.; Buffet, J.-C.; O'Hare, D. Silica@layered double hydroxide core-shell hybrid materials. *Dalton Trans.* **2018**, *47* (1), 143−149.
(48) Chen, C.; Byles, C. F. H.; Buffet, J.-C.; Rees, N. H.; Wu, Y.; O'Hare, D. Core-shell zeolite@aqueous miscible organic-layered double hydroxides. *Chem. Sci.* **2016**, *7* (2), 1457−1461.
(49) Lyu, M.; Chen, C. P.; Buffet, J.-C.; O'Hare, D. A facile synthesis of layered double hydroxide based core@shell hybrid materials. *New J. Chem.* **2020**, *44* (24), 10095−10101.
(50) Buffet, J.-C.; Byles, C. F.; Felton, R.; Chen, C.; O'Hare, D. Metallocene supported core@LDH catalysts for slurry phase ethylene polymerisation. *Chem. Commun.* **2016**, *52* (21), 4076−4079.
(51) Chen, C.; Wangriya, A.; Buffet, J.-C.; O'Hare, D. Tuneable ultra high specific surface area Mg/Al-CO3 layered double hydroxides. *Dalton Trans.* **2015**, *44* (37), 16392−16398.
(52) Shannon, R. D. Revised effective ionic radii and systematic studies of interatomic distances in halides and chalcogenides. *Acta Crystallogr.* **1976**, *A32* (5), 751−767.
(53) Bellotto, M.; Rebours, B.; Clause, O.; Lynch, J.; Bazin, D.; Elkaïm, E. Hydrotalcite Decomposition Mechanism: A Clue to the

https://doi.org/10.1021/acs.macromol.1c02604
Macromolecules 2022, 55, 3408−3414

Structure and Reactivity of Spinel-like Mixed Oxides. *J. Phys. Chem.* **1996**, *100* (20), 8535−8542.
(54) Yang, W.; Kim, Y.; Liu, P. K. T.; Sahimi, M.; Tsotsis, T. T. A study by in situ techniques of the thermal evolution of the structure of a Mg−Al−CO3 layered double hydroxide. *Chem. Eng. Sci.* **2002**, *57* (15), 2945−2953.
(55) Yu, G. Y.; Zhou, Y. H.; Yang, R.; Wang, M.; Shen, L.; Li, Y. H.; Xue, N. H.; Guo, X. F.; Ding, W. P.; Peng, L. M. Dehydration and Dehydroxylation of Layered Double Hydroxides: New Insights from Solid-State NMR and FT-IR Studies of Deuterated Samples. *J. Phys. Chem. C* **2015**, *119* (22), 12325−12334.
(56) Rhinehart, J. L.; Brown, L. A.; Long, B. K. A robust Ni(II) alpha-diimine catalyst for high temperature ethylene polymerization. *J. Am. Chem. Soc.* **2013**, *135* (44), 16316−9.
(57) Chen, Z.; Mesgar, M.; White, P. S.; Daugulis, O.; Brookhart, M. Synthesis of Branched Ultrahigh-Molecular-Weight Polyethylene Using Highly Active Neutral, Single-Component Ni(II) Catalysts. *ACS Catal.* **2015**, *5* (2), 631−636.
(58) Dai, S.; Chen, C. Direct Synthesis of Functionalized High-Molecular-Weight Polyethylene by Copolymerization of Ethylene with Polar Monomers. *Angew. Chem., Int. Ed.* **2016**, *55* (42), 13281−13285.
(59) Kenyon, P.; Mecking, S. Pentafluorosulfanyl Substituents in Polymerization Catalysis. *J. Am. Chem. Soc.* **2017**, *139* (39), 13786−13790.
(60) Kenyon, P.; Worner, M.; Mecking, S. Controlled Polymerization in Polar Solvents to Ultrahigh Molecular Weight Polyethylene. *J. Am. Chem. Soc.* **2018**, *140* (21), 6685−6689.
(61) Tran, Q. H.; Brookhart, M.; Daugulis, O. New Neutral Nickel and Palladium Sandwich Catalysts: Synthesis of Ultra-High Molecular Weight Polyethylene (UHMWPE) via Highly Controlled Polymerization and Mechanistic Studies of Chain Propagation. *J. Am. Chem. Soc.* **2020**, *142* (15), 7198−7206.
(62) Guo, L.; Dai, S.; Sui, X.; Chen, C. Palladium and Nickel Catalyzed Chain Walking Olefin Polymerization and Copolymerization. *ACS Catal.* **2016**, *6* (1), 428−441.
(63) Zhou, J.; Lancaster, S. J.; Walker, D. A.; Beck, S.; Thornton-Pett, M.; Bochmann, M. Synthesis, structures, and reactivity of weakly coordinating anions with delocalized borate structure: the assessment of anion effects in metallocene polymerization catalysts. *J. Am. Chem. Soc.* **2001**, *123* (2), 223−37.
(64) Chen, M. C.; Marks, T. J. Strong ion pairing effects on single-site olefin polymerization: mechanistic insights in syndiospecific propylene enchainment. *J. Am. Chem. Soc.* **2001**, *123* (47), 11803−4.
(65) Chen, M. C.; Roberts, J. A.; Marks, T. J. Marked counteranion effects on single-site olefin polymerization processes. Correlations of ion pair structure and dynamics with polymerization activity, chain transfer, and syndioselectivity. *J. Am. Chem. Soc.* **2004**, *126* (14), 4605−25.
(66) Roberts, J. A.; Chen, M. C.; Seyam, A. M.; Li, L.; Zuccaccia, C.; Stahl, N. G.; Marks, T. J. Diverse stereocontrol effects induced by weakly coordinating anions. Stereospecific olefin polymerization pathways at archetypal C(s)- and C(1)-symmetric metallocenium catalysts using mono- and polynuclear halo-perfluoroarylmetalates as cocatalysts. *J. Am. Chem. Soc.* **2007**, *129* (42), 12713−33.
(67) Parveen, R.; Cundari, T. R.; Younker, J. M.; Rodriguez, G. Computational Assessment of Counterion Effect of Borate Anions on Ethylene Polymerization by Zirconocene and Hafnocene Catalysts. *Organometallics* **2020**, *39* (11), 2068−2079.
(68) Ghiotto, F.; Pateraki, C.; Severn, J. R.; Friederichs, N.; Bochmann, M. Rapid evaluation of catalysts and MAO activators by kinetics: what controls polymer molecular weight and activity in metallocene/MAO catalysts? *Dalton Trans.* **2013**, *42* (25), 9040−9048.
(69) Moura, H. M.; Gibbons, N. L.; Miller, S. A.; Pastore, H. O. 2D-aluminum-modified solids as simultaneous support and cocatalyst for in situ polymerizations of olefins. *J. Catal.* **2018**, *362*, 129−145.
(70) Tymińska, N.; Zurek, E. DFT-D Investigation of Active and Dormant Methylaluminoxane (MAO) Species Grafted onto a Magnesium Dichloride Cluster: A Model Study of Supported MAO. *ACS Catal.* **2015**, *5* (11), 6989−6998.
(71) Kenyon, P.; Leung, D. W. J.; Lyu, M.; Chen, C.; Turner, Z. R.; Buffet, J.-C.; O'Hare, D. Controlling the activity of an immobilised molecular catalyst by Lewis acidity tuning of the support. *J. Catal.* **2021**, *402*, 94−100.
(72) Prinetto, F.; Ghiotti, G.; Durand, R.; Tichit, D. Investigation of Acid−Base Properties of Catalysts Obtained from Layered Double Hydroxides. *J. Phys. Chem. B* **2000**, *104* (47), 11117−11126.

https://doi.org/10.1021/acs.macromol.1c02604
Macromolecules 2022, 55, 3408−3414